Supplementary References

1. Larsen RD, Ernst LK, Nair RP, et al. Molecular cloning, sequence, and expression of a human GDP-L-fucose:β-D-galactoside 2-α-L-fucosyltransferase cDNA that can form the H blood group antigen. Proc Natl Acad Sci USA 1990;87:6674–6678.
2. Kelly RJ, Ernst LK, Larsen RD, et al. Molecular basis for H blood group deficiency in Bombay (O_h) and para-Bombay individuals. Proc Natl Acad Sci USA 1994;91:5843–5847.
3. Kelly RJ, Rouquier S, Giorgi D, et al. Sequence and expression of a candidate for the human *secretor* blood group α(1,2)fucosyltransferase gene (FUT2). J Biol Chem 1995;270:4640–4649.
4. Kukowska-Latallo J, Larsen RD, Nair RP, et al. A cloned human cDNA determines expression of a mouse stage-specific embryonic antigen and the Lewis blood group α(1,3/1,4)fucosyltransferase. Genes Dev 1990;4:1288–1303.
5. Lowe JB, Stoolman LM, Nair RP, et al. ELAM-1-dependent cell adhesion to vascular endothelium determined by a transfected human fucosyltransferase cDNA. Cell 1990;63:475–484.
6. Goelz SE, Hession C, Goff D, et al. ELFT: a gene that directs the expression of an ELAM-1 ligand. Cell 1990;63:1349–1356.
7. Weston BW, Nair RP, Larsen RD, et al. Isolation of a novel human α(1,3)fucosyltransferase gene and molecular comparison to the human Lewis blood group α(1,3/1,4)fucosyltransferase gene. J Biol Chem 1992;267:4152–4160.
8. Weston BW, Smith PL, Kelly RJ, et al. Molecular cloning of a fourth member of a human α(1,3)fucosyltransferase gene family. J Biol Chem 1992;267:24575–24584.
9. Sasaki K, Kurata K, Funayama K, et al. Expression cloning of a novel α1,3-fucosyltransferase that is involved in biosynthesis of the sialyl Lewis x carbohydrate determinants in leukocytes. J Biol Chem 1994;269:14730–14737.
10. Natsuka S, Gersten KM, Zenita K, et al. Molecular cloning of a cDNA encoding a novel human leukocyte α-1,3-fucosyltransferase capable of synthesizing the sialyl Lewis x determinants. J Biol Chem 1994;269:16789–16794.
11. Yanagidani S, Uozumi N, Ihara Y, et al. Purification and cDNA cloning of GDP-L-Fuc:*N*-acetyl-β-D-glucosaminide:α1-6 fucosyltransferase (α1-6 FucT) from human gastric cancer MKN45 cells. J Biochem 1997;121:626–632.
12. Yamamoto F, Marken J, Tsuji T, et al. Cloning and characterization of DNA complementary to human UDP-GalNAc: Fucα1→2Gal α1→3GalNac transferase (histo-blood group A transferase) mRNA. J Biol Chem 1990;265:1146–1151.
13. Yamamoto F, Clausen H, White T, et al. Molecular genetic basis of the histo-blood group ABO system. Nature 1990;345:229–233.
14. Xu H, Storch T, Yu M, et al. Characterization of the human Forssman synthetase gene. J Biol Chem 1999;274:29390–29398.
15. Okajima T, Nakamura Y, Uchikawa M, et al. Expression cloning of human globoside synthase cDNAs. J Biol Chem 2000;275:40498–40503.
16. Hiruma T, Togayachi A, Okamura K, et al. A novel human β1,3-*N*-acetylgalactosaminyltransferase that synthesizes a unique carbohydrate structure, GalNAcβ1-3GlcNAc. J Biol Chem 2004;279:14087–14095.
17. Nagata Y, Yamashiro S, Yodoi J, et al. Expression cloning of β1,4 *N*-acetyltransferase cDNAs that determine the expression of G_{M2} and G_{D2} gangliosides. J Biol Chem 1992;267:12082–12089.
18. Montiel MD, Krzewinski-Recchi MA, Delannoy P, et al. Molecular cloning, gene organization and expression of the human UDP-GalNAc:Neu5Acα2-3Galβ-R β1,4-*N*-acetylgalactosaminyltransferase responsible for the biosynthesis of the blood group Sd^a/Cas antigen: evidence for an unusual extended cytoplasmic domain. Biochem J 2003;373:369–379.
19. Sato T, Gotoh M, Kiyohara K, et al. Molecular cloning and characterization of a novel human β1,4-*N*-acetylgalactosaminyltransferase, β4GalNAc-T3, responsible for the synthesis of *N,N'*-diacetyllactosediamine, GalNacβ1-4GlcNAc. J Biol Chem 2003;278:47534–47544.
20. Gotoh M, Sato T, Kiyohara K, et al. Molecular cloning and characterization of β1,4-*N*-acetylgalactosaminyltransferases IV synthesizing *N,N'*-diacetyllactosamine. FEBS Lett 2004;562:134–140.
21. Bierhuizen MFA, Fukuda M. Expression cloning of a cDNA encoding UDP-GlcNAc:Galβ1-3-GalNAc-R (GlcNAc to GalNAc) β1-6GlcNAc transferase by gene transfer into CHO cells expressing polyoma large tumor antigen. Proc Natl Acad Sci USA 1992;89:9326–9330.
22. Yeh JC, Ong E, Fukuda M. Molecular cloning and expression of novel β1-6-*N*-acetylglucosaminyltransferase that forms core 2, core 4, and I branches. J Biol Chem 1999;274:3215–3221.
23. Schwientek T, Yeh JC, Levery SB, et al. Control of *O*-glycan branch formation. Molecular cloning and characterization of a novel thymus-associated core 2 β1-6-*N*-acetylglucosaminyltransferase. J Biol Chem 2000;275:11106–11113.
24. Kitagawa H, Paulson JC. Differential expression of five sialyltransferase genes in human tissues. J Biol Chem 1994;269:17872–17878.
25. Kim YJ, Kin KS, Kim SH, et al. Molecular cloning and expression of human Gal β 1,3GalNAc α 2,3-sialyltransferase (hST3Gal II). Biochem Biophys Res Commun 1996;228:324–327.
26. Kitagawa H, Paulson JC. Cloning and expression of human Gal β 1,3(4)GlcNAc α 2,3-sialyltransferase. Biochem Biophys Res Commun 1993;194:375–382.
27. Sasaki K, Watanabe E, Kawashima K, et al. Expression cloning of a novel Galb(1-3/1-4)GlcNAc a2,3-sialyltransferase using lectin resistance selection. J Biol Chem 1993;268:22782–22787.
28. Ishii A, Ohta M, Watanabe Y, et al. Expression cloning and functional characterization of human cDNA for ganglioside G_{M3} synthase. J Biol Chem 1998;273:31652–31655.
29. Okajima T, Fukumoto S, Miyazaki, H, et al. Molecular cloning a novel α 2,3-sialyltransferase (ST3Gal VI) that sialylates type II lactosamine structures on glycoproteins and glycolipids. J Biol Chem 1999;274:11479–11486.
30. Grundmann U, Nerlich C, Rein T, et al. Complete cDNA sequence encoding human β-galactoside α-2,6-sialyltransferase. Nucleic Acids Res 1990;18:667.
31. Takashima S, Tsuji S, Tsujimoto M. Characterization of the second type of human β-galactoside α2,6-sialyltransferase (ST6Gal II), which sialylates Galβ1,4GlcNAc structures on oligosaccharides preferentially. J Biol Chem 2002;277:45719–45728.
32. Ikehara Y, Kojima N, Kurosawa N, et al. Cloning and expression of a human gene encoding an *N*-acetylgalactosamine-α2,6-sialyltransferase (ST6GalNAc I): a candidate for synthesis of cancer-associated sialyl-Tn antigens. Glycobiology 1999;9:1213–1224.
33. Samyn-Petit B, Krzewinski-Recchi MA, Steelant WF, et al. Molecular cloning and functional expression of human ST6GalNAc II. Molecular expression in various human cultured cells. Biochim Biophys Acta 2000;1474:201–211.
34. Tsuchida A, Ogiso M, Nakamura Y, et al. Molecular cloning and expression of human ST6GalNAc III: restricted tissue distribution and substrate specificity. J Biochem 2005;138:237–243.
35. Harduin-Lepers A, Stokes DC, Steelant WFA, et al. Cloning, expression and gene organization of a human Neu5Acα2-3Galβ1-3GalNAc α2,6-sialyltransferase: hST6GalNAc IV. Biochem J 2000;352:37–48.
36. Okajima T, Fukumoto S, Ito H, et al. Molecular cloning of brain-specific GD1α synthase (ST6GalNAc V) containing CAG/glutamine repeats. J Biol Chem 1999;274:30557–30562.
37. Okajima T, Chen HH, Ito H, et al. Molecular cloning and expression of mouse GD1α/GD1aα/GQ1bα synthase (ST6GalNAc VI) gene. J Biol Chem 2000;275:6717–6723.

38. Ohtake S, Ito Y, Fukuta M, et al. Human N-acetylgalactosamine 4-sulfate 6-O-sulfotransferase cDNA is related to human B cell recombination activating gene-associated gene. J Biol Chem 2001;276:43894–43900.
39. Fukuta M, Inazawa J, Torii T, et al. Molecular cloning and characterization of human keratan sulfate Gal-6-sulfotransferase. J Biol Chem 1997;272:32321–32328.
40. Li X, Tedder TF. CHST1 and CHST2 sulfotransferases expressed by human vascular endothelial cells: cDNA cloning, expression, and chromosomal localization. Genomics 1999; 55:345–347.
41. Fukuta M, Kobayashi Y, Uchimura K, et al. Molecular cloning and expression of human chondroitin 6-sulfotransferase. Biochim Biophys Acta 1998;1399:57–61.
42. Bistrup A, Bhakta S, Lee JK, et al. Sulfotransferases of two specificities function in the reconstitution of high endothelial cell ligands for L-selectin. J Cell Biol 1999;145:899–910.
43. Lee JK, Bhakta S, Rosen SD, et al. Cloning and characterization of a mammalian *N*-acetylglucosamine-6-transferase that is highly restricted to intestinal tissue. Biochem Biophys Res Commun 1999;263:543–549.
44. Bonten E, van der Spoel A, Fornerod M, et al. Characterization of human lysosomal neuraminidase defines the molecular basis of the metabolic storage disorder sialidosis. Genes Dev 1996;10: 3156–3169.
45. Monti E, Preti A, Rossi E, et al. Cloning and characterization of NEU2, a human gene homologous to rodent soluble sialidases. Genomics 1999;57:137–143.
46. Wada T, Yoshikawa Y, Tokuyama S, et al. Cloning, expression, and chromosomal mapping of a human ganglioside sialidase. Biochem Biophys Res Commun 1999;261:21–27.
47. Monti E, Bassi MT, Bresciani R, et al. Molecular cloning and characterization of NEU4, the fourth member of the human sialidase gene faminy. Genomics 2004;83:445–453.

Provided for non-commercial research and education use.
Not for reproduction, distribution or commercial use.

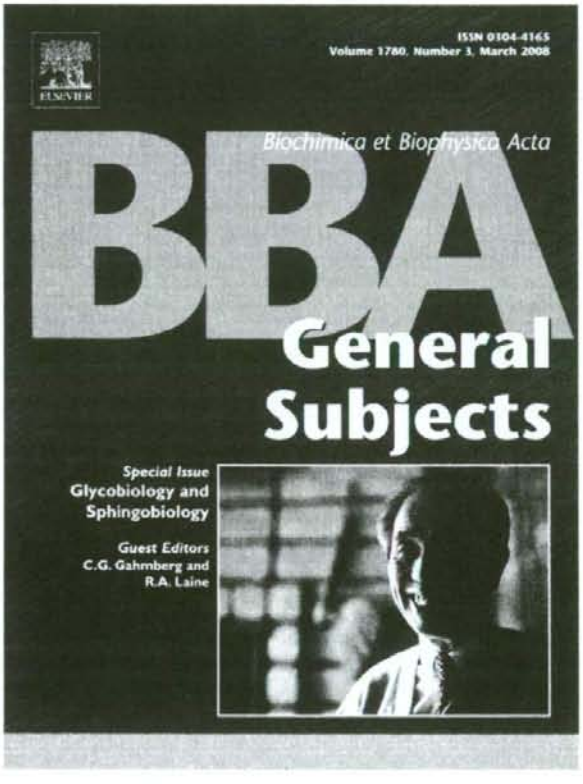

This article was published in an Elsevier journal. The attached copy is furnished to the author for non-commercial research and education use, including for instruction at the author's institution, sharing with colleagues and providing to institution administration.

Other uses, including reproduction and distribution, or selling or licensing copies, or posting to personal, institutional or third party websites are prohibited.

In most cases authors are permitted to post their version of the article (e.g. in Word or Tex form) to their personal website or institutional repository. Authors requiring further information regarding Elsevier's archiving and manuscript policies are encouraged to visit:

http://www.elsevier.com/copyright

Available online at www.sciencedirect.com
ScienceDirect
Biochimica et Biophysica Acta 1780 (2008) 467–471
Biochimica et Biophysica Acta
BBA
www.elsevier.com/locate/bbagen

Review

Incomplete synthesis of the Sd^a/Cad blood group carbohydrate in gastrointestinal cancer

Taeko Dohi *, Yuki I. Kawamura

Department of Gastroenterology, Research Institute, International Medical Center of Japan, Toyama 1-21-1, Shinjuku, Tokyo 162-8655, Japan
CREST, Tokyo, Japan

Received 14 June 2007; received in revised form 20 August 2007; accepted 31 August 2007
Available online 15 September 2007

Abstract

Cancer-associated changes in cell surface carbohydrates, including incomplete synthesis of normal carbohydrate epitopes, strongly affect malignant and metastatic potential. Here, we report that compensating for the cancer-associated loss of a single glycosyltransferase, β1,4*N*-acetylgalactosaminyltransferese T2, dramatically decreased cell surface expression of both E-selectin ligands (sialyl Lewis^x and sialyl Lewis^a). This modification was associated with elevated expression of the Sd^a carbohydrate determinant, which is expressed in normal gastrointestinal mucosa and is strikingly downregulated in cancer tissues. Loss of E-selectin ligands resulted in decreased adhesion of cancer cells to activated human endothelial cells *in vitro* and eventually suppressed metastatic potential *in vivo*.
© 2007 Elsevier B.V. All rights reserved.

Keywords: Gastric cancer; Colon cancer; Sd^a; Cad; Glycosyltransferase

1. Identification of a human gastric oxyntic mucosal glycolipid as the Sd^a/Cad blood group carbohydrate

"Incomplete synthesis" and "neo-synthesis" of carbohydrate structures in cancer tissues are important in understanding cancer-associated carbohydrate changes, as well as discovering new tumor markers and cancer treatments [1].

While verifying "neo-synthesis" of ganglioside GM2 in gastric cancer tissues, we found a band in thin-layer chromatography which was stained with anti-GM2 antibody but clearly differed from GM2. This positive band was detected only in the lipid extract from normal gastric tissue and never from cancer tissue (Fig. 1A). We have purified this glycolipid from the monosialosyl glycolipid fraction of the gastric mucosa resected for peptic ulcer and analyzed it by proton nuclear resonance, negative ion fast atom bombardment mass-spectrometry, enzymatic degradation and linkage analysis of permethylated carbohydrates. The structure was determined as GalNAcβ1-4(NeuAcα2-3)Galβ1-4GlcNAcβ1-3Galβ1-4Glc-Cer, which was identical to the glycolipid identified in Cad-positive or Sd^a(+) erythrocytes [2]. Cad is a rare erythrocyte blood group which shows strong agglutination with a lectin Dolichos biflorus [3]. Anti-Sd^a blood group sera react strongly with the Cad antigen. The serological relationship between Sd^a and Cad is extensively described by Watkins [3]. Since this structure shares three terminal sugars (GalNAcβ1-4(NeuAcα2-3)Galβ1-R) with ganglioside GM2, it was detectable using monoclonal anti-GM2 antibodies. From clones of monoclonal antibodies, we selected a few which reacted preferentially to the Cad/Sd^a glycolipid for use as anti-Sd^a monoclonal antibodies. In contrast to the Cad/Sd^a glycolipid, the amount of GM2 was elevated in cancer tissues [2]. This result suggested that the synthesis of Cad/Sd^a and GM2 are unrelated, although they have the same nonreducing terminal carbohydrate structure.

We examined the presence of the Cad/Sd^a glycolipid in various gastrointestinal tissues. In the stomach, it was consistently detected in the oxyntic mucosa, but not in antral mucosa, intestinal metaplasia, atrophic mucosa, or any types of gastric cancer (Fig. 1B and [4]). The small and large intestine express Cad/Sd^a glycolipid at lower levels than in the stomach, although the Sd^a determinant GalNAcβ1-4(NeuAcα2-3)Galβ1-4GlcNAc was reported to be abundantly expressed in the colon as glycoproteins [5,6]. In summary, the Sd^a determinant is

* Corresponding author. Tel.: +81 3 3202 7181x2861; fax: +81 3 3202 7364.
E-mail address: dohi@ri.imcj.go.jp (T. Dohi).

0304-4165/$ - see front matter © 2007 Elsevier B.V. All rights reserved.
doi:10.1016/j.bbagen.2007.08.019

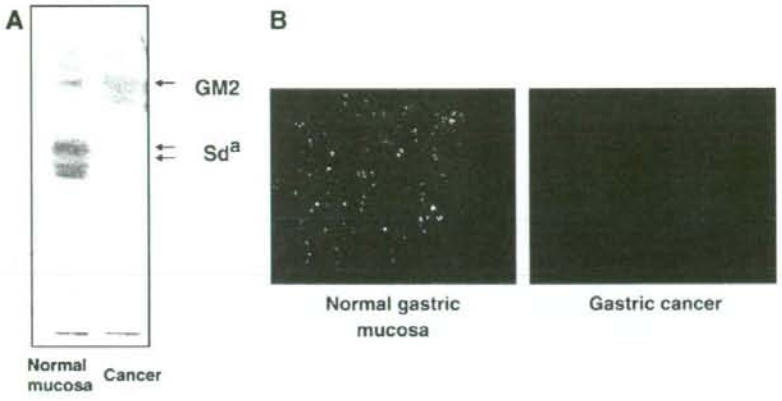

Fig. 1. Detection of the Cad/Sd^a glycolipid in the gastric mucosa. (A) Acidic glycolipid fraction extracted from 0.1 mg wet gastric mucosa tissue and gastric cancer was separated with high performance thin-layer chromatography (solvent system was chloroform:methanol:0.2% $CaCl_2$ in water, 50:40:10 by volume) and subjected to immunostaining with anti-Sd^a monoclonal antibody KM694. (B) Frozen sections of human gastric mucosa and cancer tissue were immunostained with monoclonal antibody KM694 and FITC-labelled anti-mouse IgM.

expressed abundantly in the gastrointestinal mucosa: as a glycolipid in the stomach and as glycoproteins in the colon.

To discover which oxyntic mucosa cells produced the Cad/Sd^a glycolipid, we separated epithelial cells from human stomach using a Percoll gradient. Gastric epithelial cells were grossly separated into three groups: a parietal cell rich fraction, a chief cell-rich fraction and a mucous cell rich fraction. We extracted glycolipids from each fraction and immunostained on thin-layer chromatography with an anti-Sd^a monoclonal antibody. The Cad/Sd^a glycolipid was found concentrated in the chief cell-rich fraction. The presence of this glycolipid in chief cells was also confirmed histologically by double staining with anti-Sd^a and anti-pepsinogen antibodies [7]. The functional significance of the Cad/Sd^a glycolipid in chief cells is yet to be investigated. However, its expression is notably limited in highly differentiated cells in the gastric oxyntic mucosa. Indeed, the glycolipid was not detected in any gastric or colonic cancer cell lines tested unless differentiation was artificially induced. Proliferation of the gastric cancer cell line AZ521 was suppressed by addition of the differentiation-induction reagent dimentylformamide to the culture, concomitant with elevated expression of the Cad/Sd^a glycolipid [8].

2. Biosynthesis of the Sd^a carbohydrate

To clarify the mechanism of specific expression of the Sd^a determinant, we measured the enzymatic activity. The membrane fraction from normal gastric mucosa was capable of synthesizing the Cad/Sd^a glycolipid from sialylparagloboside and UDP-GalNAc. The acceptor specificity of this fraction was determined. It efficiently transferred GalNAc to NeuAc2,3Lc4 and NeuAc2,3nLc4 in a $\beta1\rightarrow4$ linkage, but not to GM3 (Fig. 2 and [9]). Similar enzyme activity had been reported in guinea pig kidney [10], human kidney [11], colon [12], and mouse T lymphocytes [13], as a β1,4GalNAc-transferase that synthesizes the Sd^a carbohydrate determinant (Sd^a-GalNAcT). Using a mammalian expression cloning system, mouse cDNA for Sd^a-GalNAcT was cloned [14]. Based on this information, we first detected mRNA for human Sd^a-GalNAcT in the stomach, and full length cDNA was cloned later [7,15]. The β1,4GalNAcT enzyme activity was closely correlated to the levels of mRNA as determined by quantitative reverse transcriptase (RT)-PCR. As shown in the paired samples in Fig. 3, enzyme activity was strikingly decreased in all cancer tissue, in association with barely detectable mRNA levels. In the normal colon, β1,4GalNAcT activity showed a clear proximal–distal gradient as previously reported [12]. Again, enzyme activity and mRNA

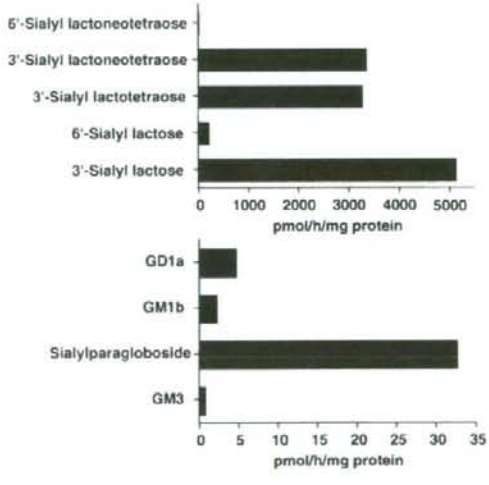

Fig. 2. Substrate specificity of β1,4GalNAcT in human gastric mucosa. Fluorescent pyridylaminated oligosaccharides (upper panel) or glycolipids (lower panel) were used as acceptors. β1,4GalNAcT activity was measured with high pressure liquid chromatography or radioactivity incorporation from UDP-[^{14}C]GalNAc. Details given in [9].

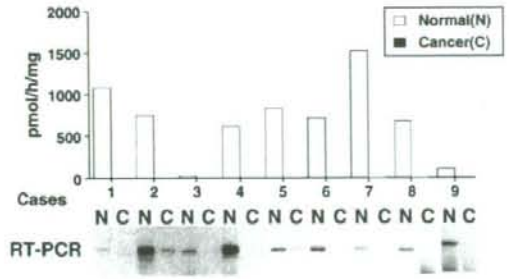

Fig. 3. Sd^a-β1,4GalNAcT enzyme activity and mRNA expression in paired samples of gastric cancer cases. Intact mucosa and cancer tissue were obtained from the same resected stomach, and enzyme activity was measured using pyridylaminated-3′-sialyl lactoneotetraose. Total mRNA was also extracted from paired tissues and subjected to RT-PCR for Sd^a-β1,4GalNAcT. An inverted photo of the electrophoresis of PCR products is shown. Sd^a-β1,4GalNAcT activity was below the detection limit in all cancer tissues.

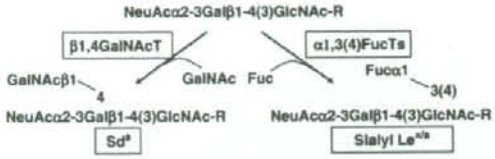

Fig. 5. Synthetic pathway of Sd^a and sialyl $Lewis^{x/a}$ carbohydrate determinants.

levels were dramatically decreased in all colon cancers (Fig. 4). Since RNA was extracted from macroscopic tumor masses, involvement of normal cells in the tumor might result in the detection of Sd^a-GalNAcT mRNA in some cancer tissues. The expression levels may not always correlate with enzyme activity, probably because it was determined by qualitative, not quantitative, RT-PCR, although we cannot exclude the possibility of the presence of another molecule that catalyzes the same reaction. However, overall results showed that decreased expression of the Sd^a/Cad glycolipid in the stomach and the Sd^a glycoprotein in the colon is attributable to low transcription levels of Sd^a-βGalNAcT.

In regards to specificity, Sd^a-GalNAcT was able to form the Sd^a determinant on both type I and type II carbohydrate chains. These acceptor oligosaccharides were also precursors of sialyl $Lewis^x$ and sialyl $Lewis^a$, respectively (Fig. 5). Sialyl $Lewis^x$ and sialyl $Lewis^a$ are synthesized by fucosyltransferase using same precursors as Sd^a-β1,4GalNAcT. They are expressed in gastrointestinal cancer as cancer-associated antigens functioning as ligands for selectin that mediate cancer metastasis. The expression of sialyl $Lewis^{x/a}$ determinants in cancer and the postoperational prognosis of patients in various cancers are significantly correlated [15–18]. Therefore, we next attempted to "normalize" incomplete synthesis of the Sd^a determinant by introducing the Sd^a-β1,4GalNAcT gene into gastric and colonic cancer cell lines.

3. Elimination of selectin ligands by introduction of Sd^a-β1,4GalNAcT

When the human gastric cancer cell line KATOIII and colon cancer cell line HT29 were stably transfected by human Sd^a-β1,4GalNAcT, cell surface expression of Sd^a increased (Fig. 6A). Transfection with Sd^a-β1,4GalNAcT also caused an almost complete loss of sialyl $Lewis^a$ and sialyl $Lewis^x$. Emergence of the Sd^a carbohydrate determinant and loss of sialyl $Lewis^a$ and sialyl $Lewis^x$ were seen in both glycolipid and glycoprotein fractions, as determined by flow cytometry (Fig. 6A), thin-layer chromatography/immunostaining and Western blotting using specific antibodies [7]. There was no difference in cell proliferation or viability between mock and Sd^a-β1,4GalNAcT transfectants. However, as expected, adhesion to endothelial cells was altered. When human umbilical vein endothelial cells (HUVEC) were activated with TNF-α, expression of E-selectin

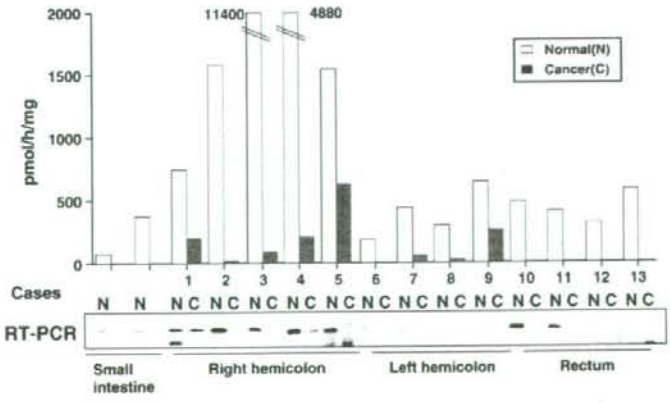

Fig. 4. Sd^a-β1,4GalNAcT enzyme activity and mRNA expression in paired samples of colonic cancer cases. Cancer tissue and adjacent intact mucosa were obtained from the same resected colon. Intact ileal mucosa was also obtained from two cases. Sd^a-β1,4GalNAcT enzyme activity was measured using pyridilaminated-3′ sialyl-lactoneotetraose. Total mRNA was also extracted from paired tissues and subjected to RT-PCR for Sd^a-β1,4GalNAcT. An inverted photo of the electrophoresis of PCR products is shown. Sd^a-β1,4GalNAcT activity was below the detection limit in all cancer tissues from cases 6, 10, 11, 12 and 13.

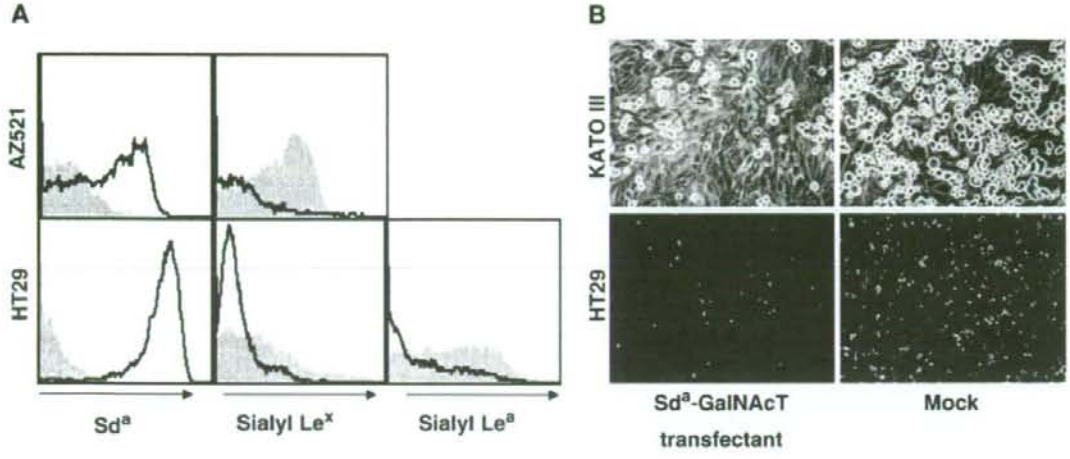

Fig. 6. Elimination of selectin ligands and reduction of adhesion to HUVEC in gastrointestinal cancer cell lines after introducing Sd^a-GalNAcT cDNA. (A) Gastric cancer cell line AZ521 or colon cancer cell line HT29 was transfected with mock-plasmid (shaded histogram) or Sd^a-β1,4GalNAcT cDNA (open histogram) and stained with anti-Sd^a monoclonal antibody KM694, anti-sialyl monoclonal antibody $Lewis^x$ KM231, or anti-sialyl $Lewis^a$ monoclonal antibody CA19-9. Surface staining was analyzed with flow cytometry. (B) Gastric cancer cell line KATO III or colon cancer cell line HT29 was transfected with Sd^a-β1,4GalNAcT cDNA or mock-plasmid. The cells were then labeled with fluorescent dye and added to the culture containing TNF-α-activated HUVEC. After incubation for 30 min and washing, microscopic photos in light field (upper panels) and dark field (lower panels) were taken.

is upregulated and the cells adhere to mock-transfected cancer cells. In contrast, many fewer Sd^a-β1,4GalNAcT transfected cells adhere to HUVEC (Fig. 6). Since adhesion of activated HUVEC to cancer cells is mediated by E-selectin, sialyl $Lewis^a$, and sialyl $Lewis^x$, induction of a single Sd^a-β1,4GalNAcT gene caused dramatic changes in cell adhesion.

4. Inhibition of tumor metastasis

We next evaluated the effects on metastatic potential of introducing the Sd^a-β1,4GalNAcT gene into gastrointestinal cancer cells. When KATO III cells are injected into the peritoneal cavity of nude mice, they formed metastatic foci in 10 weeks in the spleen, liver, peritoneum, and seminal vesicles at an incidence of 83% (10/12 mice). In contrast, Sd^a-β1,4GalNAcT transfected cells did not form any visible metastasis (0/13 mice). We also examined hematogenic metastasis of the colonic cancer cell line HT29 by counting tumor nodules 8 weeks after intrasplenic injection. Metastatic nodules were seen in all mice injected with mock-transfected cells, while only 1 out of 8 mice given Sd^a-β1,4GalNAcT-transfected HT29 cells developed liver tumors [7]. These results clearly show that the introduction of Sd^a-β1,4GalNAcT efficiently inhibited tumor metastasis in vivo.

Elimination of sialyl $Lewis^x$ and sialyl $Lewis^a$ has been an important goal in the development of new cancer therapy, and target molecules have been sought out for this purpose. However, biosynthesis of sialyl $Lewis^x$ and sialyl $Lewis^a$ involves many glycosyltransferases, including several molecular species of sialyltransferases and fucosyltransferases. In spite of extensive analyses for expression levels of these enzymes, the precise mechanisms for up-regulation of sialyl $Lewis^x$ and sialyl $Lewis^a$ have not yet been determined. In our study, we showed that introducing a single glycosyltransferase resulted in the total loss of both sialyl $Lewis^x$ and sialyl $Lewis^a$ epitopes in both glycoproteins and glycolipids. Logically, this effect should be expected in any types of cells expressing sialyl $Lewis^a$ and sialyl $Lewis^x$, irrespective of the underlying mechanism. Indeed, we succeeded in eliminating sialyl $Lewis^x$ in other gastrointestinal cancer cell lines as well as in a human leukemia cell line (our unpublished data).

5. Perspectives

Tumor resection and irradiation therapy are inevitable manipulations for cancer therapy; however, they may also increase the risk of tumor metastasis. Our approach using Sd^a-β1,4GalNAcT may be beneficial to reduce the risk of metastasis associated with these interventions. Methods for safe and efficient gene delivery are now under investigation in our laboratory.

The biological function and significance of the Sd^a carbohydrate determinant is still unknown. A secretory product of renal tubules, Tamm–Horsfall (T–H) glycoprotein, is heavily N-glycosylated and rich in the Sd^a carbohydrate determinant. A possible role has been reported for the T–H glycoprotein in protecting the distal nephron from colonization of type-S fimbriated *E. coli* (which recognize NeuAcα2,3Gal). As discussed in this paper, the addition of GalNAc to α2,3NeuAcGal may play a biological role by conformationally masking sialic acid from lectin-type molecules that recognize α2,3NeuAcGal. In the colon, where a large amount of commensal flora colonize, Sd^a-β1,4GalNAcT activity showed postnatal maturation [19]. This result might indicate a role of the Sd^a carbohydrate in epithelial–bacterial interactions. On the other hand, knowledge about molecules that recognize Sd^a is currently very limited; this

information is required to predict side effects when gene therapy using Sd^a-β1,4GalNAcT is applied.

Another important issue is the mechanisms that control Sd^a-β1,4GalNAcT gene expression. Previous work suggested that epigenetic changes (such as histone deacetylation and/or DNA methylation) are involved in the mechanism of disialyl Lewis^a loss and increased sialyl Lewis^a expression in human colon cancer [20]. It is possible that the Sd^a-GalNAcT gene is also silenced by hypermethylation in gastrointestinal cancers since treatment of a colon cancer cell line with a DNA methylation inhibitor (5-Aza-deoxycytidine) induced expression of the Sd^a carbohydrate determinant (our unpublished data). DNA hypermethylation takes place in inflammatory changes and silences a group of genes. Thus, it is important whether the Sd^a-GalNAcT gene is methylated together with other genes representing a CpG island hypermethylated phenotype. The status of Sd^a-GalNAcT in precancerous lesions associated with gastrointestinal inflammation is also of great interest.

Acknowledgements

We thank Drs. Kazuo Abe, Mieko Oshima and Reiji Kannagi for their support for starting and continuing this project, Drs. Nobuo Hanai and Kenya Shitara for providing us with monoclonal antibodies, and Rei Kawashima for her technical support. We thank Dr. Sen-itiroh Hakomori for his valuable advice and discussion.

This work was supported in part by grants and contracts from the Ministry of Education, Culture, Sports, Science, Technology (Grant-in-aid for Scientific Research on Priority Areas, Grant-in-aid for Young Scientist), CREST program of the Japan Science and Technology Agency, and the Ministry of Health, Labor, and Welfare.

References

[1] S. Hakomori, Glycosylation defining cancer malignancy: new wine in an old bottle, PNAS 99 (2002) 10231–10233.

[2] T. Dohi, S. Ohta, N. Hanai, K. Yamaguchi, M. Oshima, Sialylpentaosylceramide detected with anti-GM2 monoclonal antibody. Structural characterization and complementary expression with GM2 in gastric cancer and normal gastric mucosa, J. Biol. Chem. 265 (1990) 7880–7885.

[3] W. Watkins, Sda and Cad antigens, in: J.-P. Cartron, P. Rouger (Eds.), Blood cell biochemistry, Plenum Press, New York, 1995, pp. 351–375.

[4] T. Dohi, N. Hanai, K. Yamaguchi, M. Oshima, Localization of UDP-GalNAc:NeuAc alpha 2,3Gal-R beta 1,4(GalNAc to Gal)N-acetylgalactosaminyltransferase in human stomach. Enzymatic synthesis of a fundic gland-specific ganglioside and GM2, J. Biol. Chem. 266 (1991) 24038–24043.

[5] J.A. Morton, M.M. Pickles, R.I. Vanhegan, The Sda antigen in the human kidney and colon, Immunol. Invest. 17 (1988) 217–224.

[6] J.A. Morton, M.M. Pickles, A.M. Terry, The Sda blood group antigen in tissues and body fluids, Vox Sang. 19 (1970) 472–482.

[7] Y.I. Kawamura, R. Kawashima, R. Fukunaga, K. Hirai, N. Toyama-Sorimachi, M. Tokuhara, T. Tokuhara Shimizu, T. Shimizu, T. Dohi, Introduction of Sd(a) carbohydrate antigen in gastrointestinal cancer, Cancer Res. 65 (2005) 6220–6227.

[8] T. Dohi, M. Nakasuji, M. Oshima, Induction of the fundic mucosa-specific glycolipid with dimethylformamide in gastric-cancer cell lines, Int. J. Cancer 53 (1993) 137–140.

[9] T. Dohi, A. Nishikawa, I. Ishizuka, M. Totani, K. Yamaguchi, K. Nakagawa, O. Saitoh, S. Ohshiba, M. Oshima, Substrate specificity and distribution of UDP-GalNAc:sialylparagloboside N-acetylgalactosaminyltransferase in the human stomach, Biochem. J. 288 (Pt 1) (1992) 161–165.

[10] F. Serafini-Cessi, N. Dall'Olio, N. Malagolini, Characterization of N-acetyl-beta-D-galactosaminyltransferase from guinea-pig kidney involved in the biosynthesis of Sda antigen associated with Tamm–Horsfall glycoprotein. Carbohydr. Res. 151 (1986) 65–76.

[11] F. Piller, D. Blanchard, M. Huet, J.P. Cartron, Identification of a alpha-NeuAc-(2-3)-beta-D-galactopyranosyl N-acetyl-beta-D-galactosaminyltransferase in human kidney, Carbohydr. Res. 149 (1986) 171–184.

[12] N. Malagolini, F. Dall'Olio, G. Di Stefano, F. Minni, D. Marrano, F. Serafini-Cessi, Expression of UDP-GalNAc:NeuAc alpha 2,3Gal beta-R beta 1,4(GalNAc to Gal) N-acetylgalactosaminyltransferase involved in the synthesis of Sda antigen in human large intestine and colorectal carcinomas, Cancer Res. 49 (1989) 6466–6470.

[13] A. Conzelmann, S. Kornfeld, A murine cytotoxic T lymphocyte cell line resistant to *Vicia villosa* lectin is deficient in UDP-GalNAc:beta-galactose beta 1,4-N-acetylgalactosaminyltransferase, J. Biol. Chem. 259 (1984) 12536–12542.

[14] P.L. Smith, J.B. Lowe, Molecular cloning of a murine N-acetylgalactosamine transferase cDNA that determines expression of the T lymphocyte-specific CT oligosaccharide differentiation antigen, J. Biol. Chem. 269 (1994) 15162–15171.

[15] N. Futamura, S. Nakamura, M. Tatematsu, Y. Yamamura, R. Kannagi, H. Hirose, Clinicopathologic significance of sialyl Le(x) expression in advanced gastric carcinoma, Br. J. Cancer 83 (2000) 1681–1687.

[16] S.D. Hoff, Y. Matsushita, D.M. Ota, K.R. Cleary, T. Yamori, S. Hakomori, T. Irimura, Increased expression of sialyl-dimeric LeX antigen in liver metastases of human colorectal carcinoma, Cancer Res. 49 (1989) 6883–6888.

[17] S. Nakamori, M. Kameyama, S. Imaoka, H. Furukawa, O. Ishikawa, Y. Sasaki, T. Kabuto, T. Iwanaga, Y. Matsushita, T. Irimura, Increased expression of sialyl Lewisx antigen correlates with poor survival in patients with colorectal carcinoma: clinicopathological and immunohistochemical study, Cancer Res. 53 (1993) 3632–3637.

[18] T. Nakayama, M. Watanabe, T. Katsumata, T. Teramoto, M. Kitajima, Expression of sialyl Lewis(a) as a new prognostic factor for patients with advanced colorectal carcinoma, Cancer 75 (1995) 2051–2056.

[19] F. Dall'Olio, N. Malagolini, G. Di Stefano, M. Ciambella, F. Serafini-Cessi, Postnatal development of rat colon epithelial cells is associated with changes in the expression of the beta 1,4-N-acetylgalactosaminyltransferase involved in the synthesis of Sda antigen of alpha 2,6-sialyltransferase activity towards N-acetyl-lactosamine. Biochem. J. 270 (1990) 519–524.

[20] K. Miyazaki, K. Ohmori, M. Izawa, T. Koike, K. Kumamoto, K. Furukawa, T. Ando, M. Kiso, T. Yamaji, Y. Hashimoto, A. Suzuki, A. Yoshida, M. Takeuchi, R. Kannagi, Loss of disialyl Lewis^a, the ligand for lymphocyte inhibitory receptor sialic acid-binding immunoglobulin-like lectin-7 (Siglec-7) associated with increased sialyl Lewis^a expression on human colon cancers, Cancer Res. 64 (2004) 4498–4505.

Jpn. J. Infect. Dis., 61, 157-160, 2008

Short Communication

H5N1-Infected Cells in Lung with Diffuse Alveolar Damage in Exudative Phase from a Fatal Case in Vietnam

Nguyen Thanh Liem, Noriko Nakajima[1], Le Phuc Phat**, Yuko Sato[1], Hoang Ngoc Thach, Pham Viet Hung, Luong Thi San, Harutaka Katano[1], Toshio Kumasaka[1,2], Teruaki Oka[3], Shoji Kawachi[4], Takeji Matsushita[3], Tetsutaro Sata[1], Koichiro Kudo[4] and Kazuo Suzuki[1,5]*

The National Hospital of Pediatrics, Hanoi, Vietnam; [1]National Institute of Infectious Diseases, Tokyo 162-8640; [2]Juntendo University School of Medicine, Tokyo 113-8421; [3]Kanto Central Hospital, Tokyo 158-8531; [4]International Medical Center of Japan, Tokyo 162-8655; and [5]Chiba University Graduate School of Medicine, Chiba 260-8670, Japan

(Received October 23, 2007. Accepted February 4, 2008)

SUMMARY: Necropsied lung tissues of three fatal cases with avian influenza A virus (H5N1) infection in Vietnam were analyzed to detect H5N1 virus-infected cells. Formalin-fixed and paraffin-embedded lung tissue sections showed typical histological features of diffuse alveolar damage (DAD) in all cases. Immunohistochemistry for the influenza A virus nucleoprotein antigen revealed positive signals of bronchiolar and alveolar epithelial cells in only one patient, who exhibited DAD with an exudative phase and died on the 6th day after onset. However, no signal was detected in the other two cases of DAD with a proliferative phase. These patients died on day 16 and day 17 after onset, respectively. H5N1 virus antigens were detected predominantly in epithelial cells in terminal bronchioles and in alveoli, i.e., type I and type II alveolar pneumocytes, and in alveolar macrophages. The pathogenesis of exudative DAD caused by H5N1 infection is discussed.

Highly pathogenic avian influenza A H5N1 virus (H5N1) infection has been reported to cause severe respiratory disease. In 1997, H5N1 was first isolated in Hong Kong from tracheal aspirates of a 3-year-old boy with a fatal respiratory illness (1-3). In 2003, human disease associated with H5N1 re-emerged (4). Since then, the number of confirmed fatal human H5N1-infected cases has increased and now totals approximately 200 cases. These cases occurred, predominantly, in Vietnam, Thailand, and Indonesia (5-9). The histopathological data for H5N1 virus infection in humans were, however, limited (3,4,6,8,10-12), and the pathogenesis of the disease remains unclear. Examination of ex vivo infected lung tissues showed that influenza A virus nucleoprotein (InfA-NP) was detected in pneumocytes and in alveolar macrophages (13). Also the pattern of viral attachment in human respiratory tract sections showed that H5N1 attached to the apical cell membrane of bronchiolar cells, type II pneumocytes and alveolar macrophages (14,15). The postmortem study of H5N1-infected patients has recently been published for the first time (16).

In the present study, we describe the histopathological findings from three fatal cases of H5N1 infection from the National Hospital of Pediatrics in Hanoi, Vietnam. The detailed clinical findings of Case 1 and Case 2 have been described previously (5). On admission, all patients presented with fever, cough, and dyspnea, and H5N1 virus was detected in tracheal fluids by reverse-transcriptase polymerase chain reaction (RT-PCR) before death occurred. The duration of the disease in Case 1, 6 days, was much shorter than in the other two cases (Table 1). Small pieces of lung tissues in the lower respiratory tract were necropsied and histological and immunohistochemical examinations were carried out on formalin-fixed and paraffin-embedded lung tissues.

The hematoxylin and eosin-stained lung sections of Case 1 demonstrated typical histological features of diffuse alveolar damage (DAD) with an exudative phase (Fig. 1a). Eosinophilic hyaline membrane was found on alveolar ducts and on alveoli. The alveolar space was filled with proteinaceous exudates containing erythrocytes, macrophages, and cell debris. The alveolar septa were thickened by edema with mild inflammatory infiltration, consisting of lymphocytes and macrophages. In Cases 2 and 3, hyaline membrane formation was focally found, and the proliferation of fibroblasts in the interstitial space was marked in comparison to Case 1. Mild interstitial inflammation and proliferation of type II pneumocytes with bizarre and cuboidal features were observed (Fig. 1c), indicating that Cases 2 and 3 were in the proliferative (repair) phase of DAD. Squamous cell metaplasia in the bronchiolar epithelium was also observed (Fig. 1d). Focal accumulation of neutrophils in the alveolar space was found in Case 3, suggesting pulmonary bacterial infection. These histological features were similar to those reported previously in fatal human H5N1 influenza A virus-infected cases (4,8,10,11).

To detect the influenza A virus antigen, the sections were immunostained with an avidin-biotin complex immunoperoxidase method (LSAB2 kit/HRP/DAB; Dako Cytomation, Copenhagen, Denmark) using a mouse monoclonal antibody against InfA-NP (17). Positive signals for InfA-NP were detected in 6 of 6 blocks of lung tissue from Case 1, whereas they were not found in those from Case 2 or 3. The signals were found mainly in alveolar epithelial cells and in interstitial cells (Fig. 1b). The many positive cells were interpreted as type II pneumocytes and/or alveolar macrophages, but the positive cell presented in the inset in Fig. 1b was considered to be a type I pneumocyte based on its histological location and morphology. H5N1-RNA was also detected by real-time RT-

*Corresponding author: Mailing address: Chiba University Graduate School of Medicine, Inohana 1-8-1, Chuo-ku, Chiba 260-8670, Japan. Tel: +81-43-221-0831, Fax: +81-43-221-0832, E-mail: ksuzuki@faculty.chiba-u.jp

**Deceased after the contribution of this study.

Table 1. Histopathological findings in the lung of H5N1 fatal cases in Vietnam

Case	Age (y)/ Sex	Days from onset to death	Histology in lung sections	RT-PCR for H5N1 (tracheal fluids)	RT-PCR for H5N1 (paraffin-embedded sections of lung)	Immunohistochemistry for InfA-NP antigen and co-localization with cell marker proteins
1[1]	12/F	6	DAD with an exudative phase, Hyaline membrane formation Hemmorhagic necrosis	Positive	Positive	Positive for InfA-NP antigen, and colocalized with AE1/AE3, EMA, SPA, SPD, CD68, CD34
2[2]	5/M	17	DAD with a proliferative (repair) phase Hyaline membrane formation	Positive	Negative	Negative for InfA-NP antigen
3	4/M	16	DAD with a proliferative (repair) phase Hyaline membrane formation Microabscess	Positive	Negative	Negative for InfA-NP antigen

[1]: Patient 1 in Ref (5).
[2]: Patient 2 in Ref (5).
M, male; F, female; DAD, diffuse alveolar damage; InfA-NP, influenza virus A nucleoprotein; EMA, epithelial membrane antigen; SPA, surfactant protein A; SPD, surfactant protein D.

Table 2. Antibodies used for double immunofluorescence staining

Antigen	Antibody type	Stained cells	Source
cytokeratin (AE1/AE3)	mouse monoclonal	epithelial cell of bronchiole	Dako
epithelial membrane antigen (EMA)	mouse monoclonal	epithelial cell	Dako
surfactant apoprotein A (SPA)	mouse monoclonal	type II alveolar pneumocyte	Dako
surfactant apoprotein D (SPD)	rabbit polyclonal	type II alveolar pneumocyte	Chemicon[1]
CD68 (KP1)	mouse monoclonal	alveolar macrophage	Dako
CD68 (PG-M1)	mouse monoclonal	alveolar macrophage	Dako
CD34	mouse monoclonal	endothelial cell	Immunotech[2]
influenza A virus nucleoprotein	mouse monoclonal	influenza A virus infected cell	in-house Ref. (17)
influenza A virus nucleoprotein	rabbit polyclonal	influenza A virus infected cell	in-house Ref. (17)

[1]: Chemicon, Temecula, Calif., USA.
[2]: Immunotech, Marseille, France.

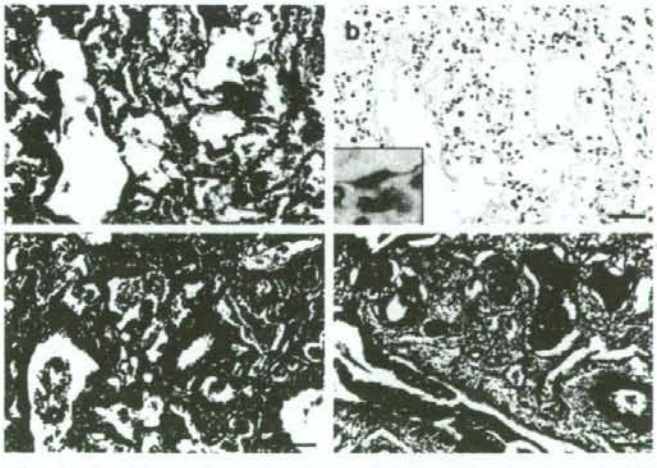

Fig. 1. Hematoxylin and eosin stainings and immunohistochemistry for influenza virus A nucleoprotein (InfA-NP) in Case 1. (a) Hyaline membrane formation is observed on the alveolar walls. In the interstitial space, edema and mild inflammatory cell infiltrates are observed (Case 1). (b) InfA-NP antigens are detected in alveolar epithelial cells and in the interstitial space. InfA-NP-positive, type I pneumocyte is indicated in the inset. (c) Mild interstitial inflammation and proliferation of type II pneumocytes with bizarre and cuboidal features were observed (Case 3). (d) Squamous cell metaplasia in the bronchiolar epithelium was also observed (Case 2). Scale bar ≈ 100 μm.

PCR in paraffin-embedded lung sections from Case 1 only (18). In DAD with a proliferative phase, as in Cases 2 and 3, viral antigens and nucleic acids were not detected.

To characterize virus-infected cells, confocal laser scanning microscopy was used to visualize double immunofluorescence staining for InfA-NP and for cell-type specific marker proteins of epithelial cells, macrophages, and endothelial cells. The antibodies used are shown in Table 2. Alexa Fluor 568-conjugated anti-mouse or anti-rabbit IgG (Molecular Probes, Eugene, Oreg., USA) and Alexa Fluor 488-conjugated anti-rabbit or anti-mouse IgG (Molecular Probes) were used as secondary antibodies. InfA-NP signals were detected most

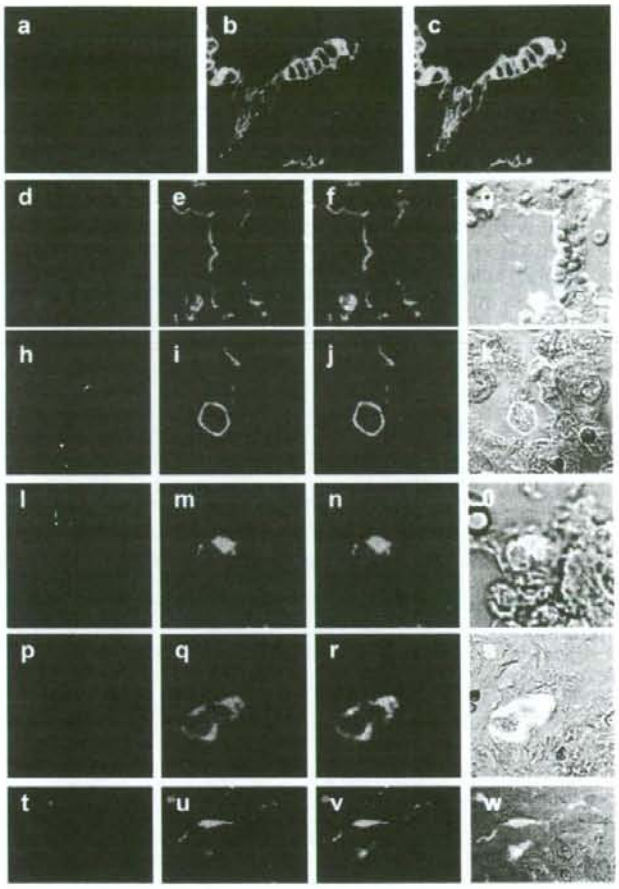

Fig. 2. The phenotype of influenza virus A nucleoprotein (InfA-NP) positive cells. InfA-NP immunoreactivity (a, d, h, l, p, t) (red color) and cytokeratin (b), EMA (e), SPD (i), CD68 (Kp1) (m), CD68 (PGM-1) (q) or CD34 (u) immunoreactivity (green color). Co-localization is presented respectively (c, f, j, n, r, v). Differential interference contrast (DIC) images are also shown (g, k, o, s, w). Original magnifications, ×400.

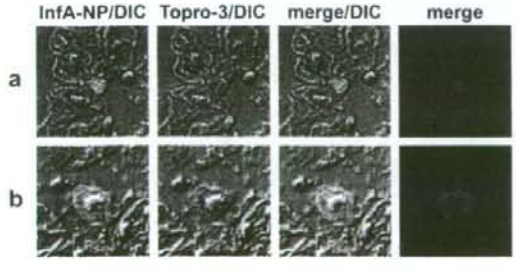

Fig. 3. Immunofluorescence staining of InfA-NP antigen in infected epithelial cells. InfA-NP immunoreactivity (red color), TO-PRO-3 nucleic acid staining (blue color) and merged images (pink color) are shown. Some were analyzed with differential interference contrast (DIC) images. The InfA-NP antigen was localized in nuclei (a) or in cytoplasm (b). Original magnifications, ×400.

frequently in epithelial (EMA-positive) cells. They were also detected in AE1/AE3, SPD, SPA, and CD68-positive cells (Fig. 2), indicating that H5N1 virus antigens were present predominantly in the epithelial cells in terminal bronchioles and alveoli, mainly in type II alveolar pneumocytes and in alveolar macrophages. A few H5N1 virus-infected type I pneumocytes were also suggested by double-positive staining for InfA-NP and for EMA, in combination with distinctive morphology. Although the number was very few, the InfA-NP signal was also detected in CD34-positive cells, suggesting that the H5N1 had infected some CD34-positive endothelial cells. Further investigation will be necessary to confirm the H5N1 infection of human endothelial cells, as has been observed in the endothelial cells of chickens and other birds (19). The localization of InfA-NP antigen within the cell was determined by counterstaining with TO-PRO-3 nucleic acid staining (Molecular Probes). Some InfA-NP signals were detected in nuclei (Fig. 3a) and others were detected in the cytoplasm (Fig. 3b). Histologically, in the early phase of infection, InfA-NP antigen was localized in the nucleus, while in the late phase of infection, InfA-NP antigen was localized in the cytoplasm (20). These observations suggested that viruses were in the proliferative stage in the early phase of H5N1 infection. The histopathological data

are summarized in Table 1.

Avian influenza viruses have been found to preferentially bind to sialic acid-α-2,3-Gal (SAα2-3)-linked oligosaccharides, while human influenza viruses were found to bind to SAα2-6-linked oligosaccharides (21), although these findings were made in vitro or ex vivo experiments. As an in vivo examination, we performed an analysis with the double-staining technique using a monoclonal antibody against InfA-NP in combination with either biotinylated *Maackia amurensis* agglutinin (MAA) lectin (Vector Laboratories, Burlingame, Calif., USA) which is specific for SAα2-3-linked oligosaccharides, or with *Sambucus nigra* agglutinin (SNA) lectin (EY Laboratories, San Mateo, Calif., USA), which is specific for SAα2-6-linked oligosaccharides. In the alveoli, many cells were not stained by SNA lectin but were stained by MAA lectin, suggesting that they express SA α 2-3-linked oligosaccharides, as found in previous reports (21). Unexpectedly, the InfA-NP-positive cells were not double-stained by MAA lectin.

Although the materials were restricted to small pieces of lung tissue in the lower respiratory tract, the evidence in the present study showed that several types of cells in the lung, namely type I and type II alveolar pneumocytes, epithelial cells in terminal bronchioles, macrophages in the alveolar space and CD34-positive endothelial cells in the interstitial tissues, were involved in the disease. The evidence in Case 1, the case with H5N1 infection who died on day 6 after onset, strongly suggests that H5N1 may infect the epithelial cells of alveolar tissues in the early clinical phase and can thereafter be transmitted to adjacent cells. The dissemination of infection among these cells was supposed to be accompanied by the release of pro-inflammatory cytokines from the infected alveolar macrophages (4,10,12), resulting in rapid progression from DAD with an exudative phase to that with a proliferative phase.

ACKNOWLEDGMENTS

This study was supported in part by grants of Ministry of Education, Culture, Sports, Science and Technology of Japan and Ministry of Health, Labour and Welfare of Japan.

REFERENCES

1. Subbarao, K., Klimov, A., Katz, J., et al. (1998): Characterization of avian influenza A (H5N1) virus isolated from a child with a fatal respiratory illness. Science, 279, 393-396.
2. Claas, E.C.J., Osterhaus, A.D.M.E., van Beek, R., et al. (1998): Human influenza A H5N1 virus related to a highly pathogenic avian influenza virus. Lancet, 351, 472-477.
3. To, K.F., Chan, P.K.S., Chan, K.F., et al. (2001): Pathology of fatal human infection associated with avian influenza A H5N1 virus. J. Med. Virol., 63, 242-246.
4. Peiris, J.S.M., Yu, W.C., Leung, C.W., et al. (2004): Re-emergence of fatal human influenza A subtype H5N1 disease. Lancet, 363, 617-619.
5. Hien, T.T., Liem, N.T., Dung, N.T., et al. (2004): Avian influenza A (H5N1) in 10 patients in Vietnam. N. Engl. J. Med., 350, 1179-1188.
6. Ungchusak, K., Auewarakul, P., Dowell, S.F., et al. (2005): Probable person-to-person transmission of avian influenza (H5N1). N. Engl. J. Med., 352, 333-340.
7. Chokephaibulkit, K., Uiprasertkul, M., Puthavathana, P., et al. (2005): A child with avian influenza A (H5N1) infection. Pediatr. Infect. Dis. J., 24, 162-166.
8. Chotpitayasunondh, T., Ungchusak, K., Hanshaoworakul, W., et al. (2005): Human disease from influenza A (H5N1), Thailand, 2004. Emerg. Infect. Dis., 11, 1036-1041.
9. World Health Organization. Confirmed human cases of avian influenza A (H5N1). Online at <http://www.who.int/csr/disease/avian_influenza/country/en/>. Accessed 4 September 2007.
10. Uiprasertkul, M., Puthavathana, P., Sangsiriwut, K., et al. (2005): Influenza A H5N1 replication sites in humans. Emerg. Infect. Dis., 11, 201-209.
11. Ng, W.F., To, K.F., Lam, W.W.L., et al. (2006): The comparative pathology of severe acute respiratory syndrome and avian influenza A subtype H5N1–a review. Hum. Pathol., 37, 381-390.
12. Uiprasertkul, M., Kitphati, R., Puthavathana, P., et al. (2007): Apoptosis and pathogenesis of avian influenza A (H5N1) virus in humans. Emerg. Infect. Dis., 13, 708-712.
13. Nicolls, J.M., Chan, M.C.W., Chan, W.Y., et al. (2007): Tropism of avian influenza A (H5N1) in the upper and lower respiratory tract. Nat. Med., 13, 147-149.
14. Riel, D.V., Munster, V.J., de Wit, E., et. al. (2006): H5N1 virus attachment to lower respiratory tract. Science, 399, 312.
15. Riel, D.V., Munster, V.J., de Wit, E., et al. (2007): Human and avian influenza viruses target different cells in the lower respiratory tract of humans and other mammals. Am. J. Pathol., 171, 1215-1222.
16. Gu, J., Xie, Z., Liu, J., et al. (2007): H5N1 infection of the respiratory tract and beyond: a molecular pathology study. Lancet, 370, 1137-1145.
17. Chen, Z., Sahashi, Y., Matsuo, K., et al. (1998): Comparison of the ability of viral protein-expressing plasmid DNAs to protect against influenza. Vaccine, 16, 1544-1549.
18. Ng, E.K.O., Cheng, P.K.C., Ng, A.Y.Y., et al. (2005): Influenza A H5N1 detection. Emerg. Infect. Dis., 11, 1303-1305.
19. Lee, C.W., Suarez, D.L., Tumpey, T.M., et al. (2005): Characterization of highly pathogenic H5N1 avian influenza A viruses isolated from south Korea. J. Virol., 79, 3692-3702.
20. Nishimura, H., Itamura, S., Iwasaki, T., et al. (2000): Characterization of human influenza A (H5N1) virus infection in mice: neuro-, pneumo- and adipotropic infection. J. Gen. Virol., 81, 2503-2510.
21. Shinya, K., Ebina, M., Yamada, S., et al. (2006): Avian flu: influenza virus receptors in the human airway. Nature, 440, 435-436.

J Pharmacol Sci

Journal of Pharmacological Sciences
©2008 The Japanese Pharmacological Society

Forum Minireview

Pharmacological Topics of Bone Metabolism: A Novel Bisphosphonate for the Treatment of Periodontitis

Hisashi Shinoda[1,*], Sadaaki Takeyama[2], Keiko Suzuki[3], Shinobu Murakami[1], and Shoji Yamada[3]

[1]*Department of Applied Pharmacology, and* [2]*Division of Dental Pharmacology, Department of Oral Biology; Tohoku University Graduate School of Dentistry, Sendai 980-8575, Japan*

[3]*Department of Dental Pharmacology, School of Dentistry, Showa University, Tokyo 142-8555, Japan*

Received December 6, 2007; Accepted January 31, 2008

Abstract. It has been reported that the pharmacological characteristics of bisphosphonates vary depending on the side chain attached to the carbon atom of the P-C-P bond. TRK-530 is a novel synthetic bisphosphonate with an anti-oxidant methylthio-phenylthio side chain. This compound has been suggested to have both anti-inflammatory and anti–bone-resorbing effects. Such a compound could be effective for the treatment of diseases with excessive bone resorption accompanied by inflammation. We have been studying this compound as a potential therapeutic agent for periodontitis. To date, we have found that 1) TRK-530 inhibited osteoclastic bone resorption in animals and in bone organ culture, 2) both systemic and topical administration of TRK-530 prevented alveolar bone loss in animals with experimental periodontitis, 3) TRK-530 prevented prostaglandin E_2 synthesis by inhibiting the expression of cyclooxygenase (COX)-2 mRNA, and 4) TRK-530 inhibited the formation of dental calculus. The above results suggest that TRK-530 might be useful for the treatment of alveolar bone loss in periodontitis.

Keywords: bisphosphonate, periodontitis, bone resorption, prostaglandin E_2, dental calculus, bone metabolism

Introduction

Bisphosphonates (BPs) are pyrophosphate analogs that can suppress osteoclastic bone resorption. These compounds are used in the treatment of metabolic bone diseases that are associated with excessive bone resorption, including osteoporosis, Paget's disease, and cancer-related diseases such as hypercalcemia, multiple myeloma, and bone metastases secondary to breast cancer and prostate cancer (1). BPs possess a P-C-P backbone, to which two side chains (R_1 and R_2) are attached. It has been reported that the pharmacological characteristics of bisphosphonates vary depending on the nature of the side chain (1 – 5).

Disodium dihydrogen-4-(methylthio) phenylthio methanebisphosphonate (TRK-530) is a novel synthetic bisphosphonate with an anti-oxidant methylthio-phenylthio group in the R_2 side chain (Fig. 1). This compound has been suggested to have both anti–bone-resorbing and anti-inflammatory effects (6 – 8). Such a compound could be effective for the treatment of diseases with excessive bone resorption accompanied by inflammation.

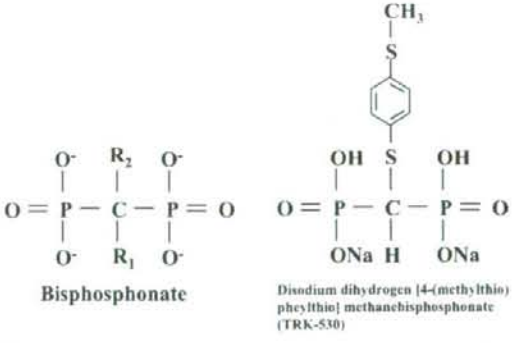

Fig. 1. Chemical structure of disodium dihydrogen-4-(methylthio) phenylthio methanebisphosphonate (TRK-530) and bisphosphonates.

*Corresponding author. shinodah@mail.tains.tohoku.ac.jp
Published onlin in J-STAGE
doi: 10.1254/jphs.FM0070272

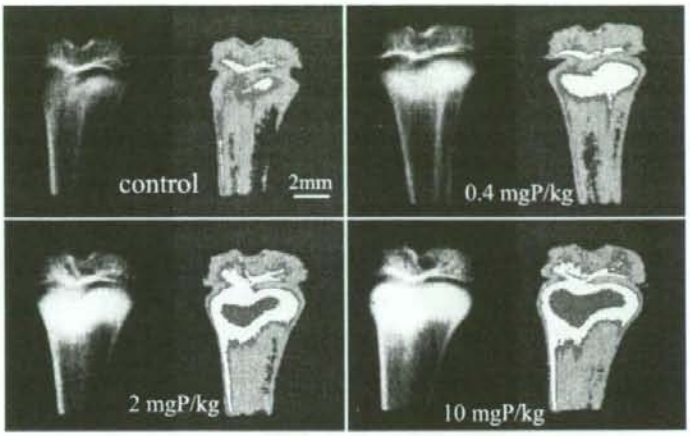

Fig. 2. Effect of subcutaneous daily injection of TRK-530 (0, 0.4, 2.0, or 10 mg/kg per day) for 7 days on the bone mineral density of tibial metaphysis in rats. Soft X-ray microradiographs (left panels) and their indexed-color images (right panels).

Periodontitis is one of the most frequent diseases in dental clinics and is characterized by excessive bone resorption and inflammation caused by plaque bacteria. We have been studying TRK-530 as a potential therapeutic agent for periodontitis. This review briefly summarizes the nature of this compound.

Inhibitory effect on bone resorption

When administered systemically, TRK-530 can increase bone mineral density in various bones in a dose-dependent fashion. Figure 2 shows soft X-ray microradiographs of the tibial metaphysis from a normal rat and from rats treated with TRK-530 (subcutaneous daily injection for 7 days). This compound, like other bisphosphonates, can block the resorption of calcified cartilage in the growth plate, subperiosteal bone, and primary spongiosa in the metaphysis, leading to a radiologically more dense structure than normal and club-shaped tibia with a decreased marrow cavity.

In organ culture of neonatal mouse calvaria, TRK-530 can inhibit bone resorption induced by various means. In fact, the effects of all the stimulators of bone resorption tested to date, including lipopolysaccharide (LPS), prostaglandin E_2 (PGE_2), interleukin (IL)-1β, and tumor necrosie factdor (TNF)-α, which have been considered to be important causal factors of alveolar bone loss in periodontitis, have been dose-dependently prevented by TRK-530. Figure 3 shows the effect of this compound on LPS-induced bone resorption in cultured mouse calvaria. In the presence of TRK-530, bone-resorbing osteoclasts over resorption lacunae were smaller, the

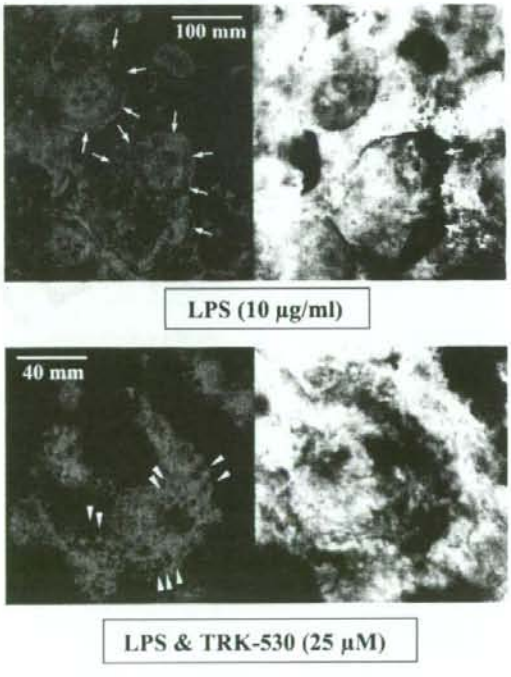

Fig. 3. Laser scanning confocal microscopic images of neonatal mouse calvaria cultured for 48 h in the presence of LPS alone (10 μg/ml) (upper panels) or in combination with TRK-530 (25 μM) (lower panels). Calvaria was stained for TRACP activity. Left panels: TRACP-positive osteoclasts and right panels: Normarsky image of corresponding site in the left panel. Arrows and arrowheads indicate the edge of resorption lacunae and cytoplasmic vacuolization, respectively.

sealing zone shown by intense tartrate-resistant acid phosphatase (TRACP) staining was diffuse, and the size and depth of resorption lacunae were reduced compared with those in calvaria cultured with LPS alone. These findings suggest that TRK-530, like other bisphosphonates (9, 10), inhibits bone resorption by inhibiting the function of osteoclasts.

Inhibitory effect on alveolar bone resorption in rats with experimental periodontitis

Previous studies have suggested that administration of BPs is effective for preventing alveolar bone loss in experimental periodontitis (11 – 14). We examined whether topical administration of TRK-530 could prevent alveolar bone loss in rats with experimental periodontitis.

Elastic rings were placed around the cervix of the right and left maxillary M_1 (first molar) to induce inflammatory periodontitis. Fifty microliters of TRK-530 solution (0 – 25 mM) was injected into the subperitoneal paratal area adjacent to the interdental area between M_1 and M_2 (second molar) on either the left or right side (control or experimental side) on day 0, 2, 4, and 6. The rats were killed on day 7. Microradiographic and histological examinations revealed that placement of the elastic ring induced severe vertical and horizontal bone resorption on the control side, while the topical administration of TRK-530 significantly prevented such alveolar bone loss on the experimental side (Fig. 4). The results suggest that administration of TRK-530 may be effective in preventing alveolar bone loss in vivo.

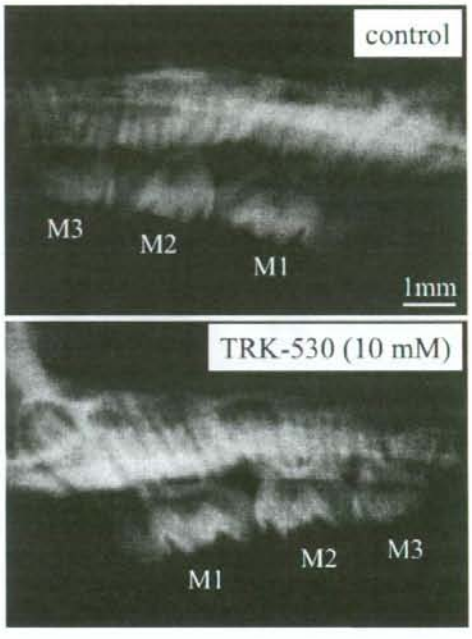

Fig. 4. Inhibitory effect of topical TRK-530 on alveolar bone loss in rats with experimental periodontitis. Placement of an elastic ring around the cervix of M_1 induced considerable recession of periodontal tissues: severe vertical and horizontal resorption of bone in the interdental area between M_1 and M_2, widening of periodontal ligament space along the roots, and irregular increase in radiolucency in the remaining alveolar bone were noted on the control side (upper panel). In the alveolar bone on the experimental side, which was injected with TRK-530 at 10 mM, these recessive changes were prevented (lower panel). M_1, M_2, and M_3: The first, second, and third molars, respectively.

Inhibitory effect on the synthesis of PGE_2

Since periodontitis is an inflammatory disease, it may be desirable to have access to a compound that could prevent inflammation in addition to bone resorption. Previous studies have shown that TRK-530 can prevent rat adjuvant arthritis that might be the result of a decrease in inflammatory cytokines such as TNF-α and neutrophil chemoattractant (CINC)-1. A decrease in serum sialic acid, a systemic parameter of inflammation, has also been reported in TRK-530–treated animals with adjuvant arthritis (7, 8). Based on these findings, we have been studying the effect of this compound on PGE_2 synthesis in organ culture of neonatal mouse calvaria. Thus far, we have found that TRK-530 (0 – 125 μM) dose-dependently prevented a LPS-stimulated increase in PGE_2 synthesis during culture (Fig. 5). The expression of cyclooxygenase (COX)-2 mRNA and COX-2 protein was also prevented. Since TRK-530 has an anti-oxidant side chain (6) and can inhibit the generation of superoxide anion that reacts with nitric oxide (NO) to form peroxynitrite ($ONOO^-$), which is known to be a potent stimulator of COX-2 expression, the inhibition of PGE_2 synthesis by TRK-530 might be, at least in part, due to the anti-oxidant nature of this compound.

Inhibitory effect on the formation of dental calculus

It is well known that a large amount of dental calculus, especially subgingival calculus, may hamper the efficacy of oral hygiene and thereby accelerate plaque formation, the accumulation of which initiates the inflammatory reaction in periodontal tissues that leads to periodontitis. Since bisphosphonates strongly bind to calcium phosphate crystals and inhibit their growth and aggregation (1), TRK-530 may have an anti-calculogenic effect in addition to its anti–bone-resorbing and anti-inflammatory effects. Therefore, using rats that were fed a

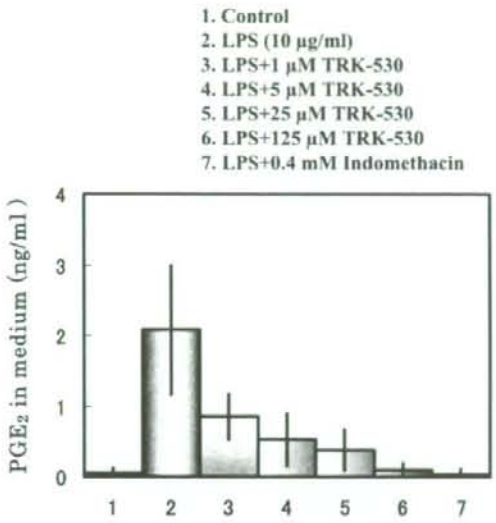

Fig. 5. Effect of (0 – 100 μM) on the synthesis of PGE_2 by neonatal mouse calvaria cultured for 72 h in the presence of LPS (10 μg/ml).

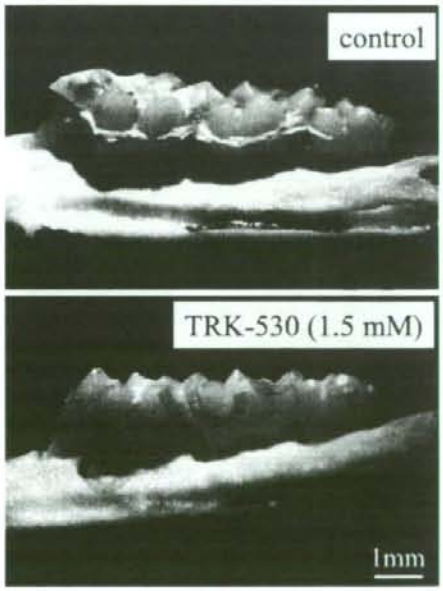

Fig. 6. Inhibitory effect of TRK-530 in drinking water on the formation of dental calculus in rats fed a calculogenic diet for 4 weeks.

calculogenic diet for 2 – 4 weeks (15), we examined whether this compound has such an effect. As expected, TRK-530 inhibited dental calculus formation in a dose-dependent fashion when it was given in drinking water (Fig. 6) (16). However, subcutaneous injection of TRK-530, at a dose that was assumed to correspond to the maximum amount of this compound absorbed from the intestine when rats received 1.5 mM TRK-530 in drinking water, did not have any significant effect, suggesting that the anticalculogenic effect of this compound was topical rather than systemic.

Conclusion

In summary, the anti–bone-resorption, anti-inflammatory, and anti-calculogenic effects of TRK-530 suggest that if an appropriate drug-delivery system can be developed, this compound might be useful clinically as a therapeutic agent for periodontitis.

References

1 Fleisch H. Bisphosphonates in bone disease. 4th ed. San Diego, San Francisco, New York, Boston, London, Sydney, Tokyo: Academic Press; 2000.
2 Shinoda H, Adamek G, Felix R, Fleisch H, Schenk R, Hagen P. Structure-activity relationships of various bisphosphonates. Calcif Tissue Int. 1983;35:87–99.
3 Geddes AD, D'Souza SM, Ebetino FH, Ibotson KJ. Bisphosphnates: structure activity relationship and therapeutic implications. Bone Miner Res. 1994;8:265–306.
4 Rogers MJ, Gordon S, Benford HL, Coxon FP, Luckman SP, Frith JC. Cellular and molecular mechanism of action of bisphosphonates. Cancer. 2000;88 Suppl:2961–2978.
5 Russell RGG. Determinants of structure-function relationships among bisphosphonates. Bone. 2007;40:S21–S25.
6 Tanahashi M, Funaba Y, Tateishi A, Kawabe N, Nakadate-Matsushita T. TRK-530 inhibits accumulation of superoxide anions derived from human polymorphonuclear leukocytes and bone-resorption induced by activated osteoclasts. Pharmacology. 1998;56:125–130.
7 Tanahashi M, Koike J, Kawabe N, Nakadate-Matsushita T. Inhibitory effect of TRK-530 on inflammatory cytokines in bone marrow of rats with adjuvant arthritis. Pharmacology. 1998;56:237–241.
8 Tanahashi M, Funaba Y, Itoh M, Kawabe N, Nakadate-Matsushita T. Inhibitory effects of TRK-530 on rat adjuvant arthritis. Pharmacology. 1998;56:242–251.
9 Suzuki K, Takeyama S, Kikuchi T, Yamada S, Sodek J, Shinoda H. Osteoclast responses to lipopolysaccharide, parathyroid hormone and bisphosphonates in neonatal murine calvaria analysed by laser scanning confocal microscopy. J Histochem Cytochem. 2005;53:1525–1537.
10 Suzuki K, Takeyama S, Sakai Y, Yamada S, Shinoda S. Current topics in pharmacological research on bone metabolism: Inhibitory effects of bisphosphonates on the differentiation and activity of osteoclasts. J Pharmacol Sci. 2006;100:189–194.
11 Brunsvold MA, Chaves ES, Komman KS, Aufdenorte TB, Wood R. Effects of bisphosphonates on experimental periodontitis in

monkeys. J Periodontol. 1992;63:825–830.
12 Shoji K, Horiuchi H, Shinoda H. Inhibitory effects of a bisphosphonate (risedronate) on experimental periodontitis in rats. J Periodont Res. 1995;30:277–284.
13 Reddy MS, Weatherfold TW, Smith CA, West BD, Jeffcoat MK, Jacks TK. Alendronate treatment of naturally-occurring periodontitis in beagle dogs. J Periodontol. 1995;66:211–217.
14 Mitsuta T, Horiuchi H, Shinoda H. Effects of topical administration of clodronate on alveolar bone resorption in rats with experimental periodontitis. J Periodontol. 2002;73:479–486.
15 Brinner WW, Francis MD, Widder JS. The control of dental calculus in experimental animals. Int Dent J. 1971;21:61–72.
16 Haq Sikder MN, Itoh M, Iwatsuki N, Shinoda H. Inhibitory effect of a novel bisphosphonate, TRK-530, on dental calculus formation in rats. J Periodontol. 2004;75:537–545.

DEVELOPMENT AND APPLICATION OF A SPECIFIC MONOCLONAL ANTIBODY FOR THYROID CANCER

Michiko Watanabe[1], Hiroshi Takeyama[2], Yoshinobu Manome[1].
[1]Department of Molecular Cell Biology, [2]Department of Surgery, Jikei University School of Medicine. 3-25-8 Nishishin-bashi, Minato-ku, Tokyo 104-8461

Thyroid cancer has been diagnosed conventionally by fine needle aspiration (FNA). However, even though the diagnostic accuracy of FNA has increased, 20% of the cases still require further investigation to determine if the lesion is benign or malignant. Other diagnostic procedures such as echography, scintigraphy, and CTscanning are of little help. Therefore, development of a more accurate system is required. A monoclonal antibody, JT95, was established by Takeyama, Watanabe and *et al.*, and it specifically reacts to human thyroid cancer. The immunohistochemical reactivity of JT95 was 96% to papillary carcinoma and 75% to follicular carcinoma, but it showed hardly any reaction to normal tissues. That specific reactivity on the 288 cases of thyroid cancer was confirmed in 13 medical facilities. The efficacy was studied under the jurisdiction of the Japanese Society of Thyroid Surgery.

This antibody recognized a glycoprotein containing sialic acid and which had a molecular weight of 250 kD. Amino-acid sequencing revealed that the antigen was glycosylated fibronectin. An approximately half-sized, 105-kD tumor-related antigen was found to be circulating in the body of the patients and was detected in the blood by an immunoblot-assay. In the serodiagnosis using an enzyme-linked immunosorbent assay, JT95 detected 80% of relapsed or metastasized thyroid cancers. In contrast, the detection rate was merely 51% in the primary patients. To improve the sensitivity and enable precise quantification, we are currently attempting to label the antibody with nano-particles. In addition, immunohistochemical investigation using the antibody contributes to the understanding of tumor antigen distribution and biological activities in thyroid diseases. Increased sensitivity of JT95 will raise the potential for use of JT95 in diagnosis and treatment. Monoclonal antibodies have become more important in both research and clinical applications. We consider that clinical use of the JT95 antibody might be another therapeutic application.

CBSM 2008

Molecular meta-strategy

― 分子レベルの診断・治療をめざす網羅的戦略 ―

The 7th Cell Biology Summer Meeting at the Kamogawa Grand Hotel, July 5th and 6th in 2008.

開催日時： 平成20年7月5日(土)～6日(日)

開催地：鴨川グランドホテル 〒296-0044 千葉県鴨川市広場820

TEL04-7092-2111 FAX04-7092-3500

＜CBSM 2008 第7回主催本部 馬目佳信 ＞

東京慈恵会医科大学総合医科学研究センターDNA医学研究所

分子細胞生物学研究部

〒105-8461 東京都港区西新橋3-25-8

TEL. 03-3433-1111 (内.2360) /FAX. 03-3578-8072

(事務局：渡辺美智子 E-mail: troy@jikei.ac.jp)

＜CBSM 代表 芝崎 太＞

(財) 東京都医学研究機構・東京都臨床医学総合研究所

がん・生活習慣病等プロジェクト

〒113-8613 東京都文京区本駒込3-18-22

TEL. 03-4463-7587 (直通) /FAX. 03-3823-0085

CBSM2008　発表プログラム

（第一日目）

第１日目:７月5日（土）

受付開始及びチェックイン：11:30 - 12:30
受付：11:30 より一階フロント前

会場：コンベンションホール（白妙の間）

12:00-12:05　開会の辞：馬目 佳信（東京慈恵会医科大学DNA医学研究所分子細胞生物学研究部）

12:05-12:10　挨拶：　芝崎　太（東京都臨床医学総合研究所）

Session 1:　アカデミック領域からの発表－１

座長：松田　浩珍　先生（東京農工大学大学院共生科学技術研究院）

オープニング講演

12:10-12:30　「医療応用を目指した蛍光半導体ナノ粒子の開発」

藤岡　宏樹　先生（東京慈恵会医科大学 DNA 医学研究所分子細胞生物学研究部）

一般演題

12:30-12:45　「アトピー性皮膚炎治療標的としてのIKK-NFκB経路の可能性」
田中あかね、松田浩珍（東京農工大学大学院共生科学技術研究院）

12:45-13:00　「A new mechanism of polyaromatic hydrocarbon response regulation in mammalian cells」
Alexander Endler , Li Chen, Futoshi Shibasaki
(Department of Biology, School of Basic Medicine, Tongji University, Shanghai, China)

Session 2:　臨床開発の立場からの発表
座長：青柳　憲和　先生（バイオ・ラッド ラボラトリーズ）

基調講演　(1)

13:00 -13:15　「臨床開発の最近の流れ」
小出　徹　先生（中外製薬株式会社　臨床開発第四部）